

# Geophysical Research Letters

## RESEARCH LETTER

10.1002/2014GL059568

### Key Points:

- Method is presented for calculating induced lithospheric electric fields
- Comparison of results is made with geoelectric field data
- Real-time algorithms can be developed from the method presented

### Correspondence to:

J. J. Love,  
jlove@usgs.gov

### Citation:

Love, J. J., and A. Swidinsky (2014), Time causal operational estimation of electric fields induced in the Earth's lithosphere during magnetic storms, *Geophys. Res. Lett.*, 41, 2266–2274, doi:10.1002/2014GL059568.

Received 10 FEB 2014

Accepted 13 MAR 2014

Accepted article online 2 APR 2014

Published online 15 APR 2014

## Time causal operational estimation of electric fields induced in the Earth's lithosphere during magnetic storms

Jeffrey J. Love<sup>1</sup> and Andrei Swidinsky<sup>2</sup>

<sup>1</sup>Geomagnetism Program, U.S. Geological Survey, Denver, Colorado, USA, <sup>2</sup>Department of Geophysics, Colorado School of Mines, Golden, Colorado, USA

**Abstract** In support of projects for monitoring geomagnetic hazards for electric power grids, we develop a simple mathematical formalism, consistent with the time causality of deterministic physics, for estimating electric fields that are induced in the Earth's lithosphere during magnetic storms. For an idealized model of the lithosphere, an infinite half-space having uniform electrical conductivity properties described by a galvanic tensor, we work in the Laplace-transformed frequency domain to obtain a transfer function which, when convolved with measured magnetic field time series, gives an estimated electric field time series. Using data collected at the Kakioka, Japan observatory, we optimize lithospheric conductivity parameters by minimizing the discrepancy between model-estimated electric field variation and that actually measured. With our simple model, we can estimate 87% of the variance in storm time Kakioka electric field data; a more complicated model of lithospheric conductivity would be required to estimate the remaining 13% of the variance. We discuss how our estimation formalism might be implemented for geographically coordinated real-time monitoring of geoelectric fields.

### 1. Introduction

A magnetic storm is the causal response of the Earth's coupled magnetospheric-ionospheric system to episodic and dynamic forcing of the solar wind [e.g., Cowley, 1995]. Analysis of the deterministic time evolution of magnetic storms [e.g., McPherron, 1991; Tsurutani *et al.*, 1997] leads to improved fundamental understanding of space physics and the nature of the Earth's surrounding space environment [e.g., Prölls, 2004]. In terms of applied science, magnetic storms represent a space weather hazard for modern technological systems [e.g., Daglis, 2004; Baker *et al.*, 2008]. Of particular concern is the storm time induction of electric fields in the Earth's electrically conducting lithosphere. These can drive uncontrolled currents in electric power grids, interfering with their operation and sometimes causing blackouts [e.g., Boteler *et al.*, 1998; Kappenman, 2012].

Ground-based monitoring is essential for operational assessment of storm time induction hazards. Magnetic observatories are now an integral part of many national and regional real-time space weather monitoring projects [e.g. Love and Finn, 2011]. Historical magnetic observatory data are used for retrospective analysis of induction hazards, and these provide a basis for extreme-event scenarios that might occur in the future [e.g., Pulkkinen *et al.*, 2012; Beggan *et al.*, 2013]. On the other hand, long historical time series measurements of geoelectric fields are scarce, and, surprisingly, those that exist are underexploited for induction-hazard research. Direct measurements of geomagnetically induced currents in grids are also useful [Bolduc, 2002; Kappenman, 2005; Watari *et al.*, 2009], but they are usually proprietary. The need to evaluate induction hazards, despite limitations of data availability, has motivated numerical modeling of induced geoelectric fields and currents [Pulkkinen *et al.*, 2007; Viljanen *et al.*, 2012; Wei *et al.*, 2013]. These models typically rely on geomagnetic variational data to simulate, as a forward problem, induction within a parameterized model of the lithosphere or, correspondingly, within a parameterized model of electric power grids.

Useful comparisons can be made with the subject of magnetotellurics, where geomagnetic and geoelectric field time series data are inverted for estimates of lithospheric electrical conductivity [e.g., Simpson and Bahr, 2005; Chave and Jones, 2012], leading to improved understanding of crustal geology and solid Earth tectonics [e.g., Korja, 2007]. Ever since early influential work [e.g., Cagniard, 1953], magnetotelluric analyses have conventionally been accomplished in the Fourier-transformed frequency domain. This reduces time domain differential equations to algebraic equations, convolution to multiplication, and time series signals to amplitudes and phases. In most cases, no return is made to the time domain, and magnetotelluric estimates of the complex impedance relationship between the magnetic and electric field data are expressed

as functions of frequency. The information content of the data often requires that magnetotelluric models of lithospheric conductivity have a fully three-dimensional distribution.

Early mathematical analyses of induction hazards were also accomplished in the Fourier frequency domain [e.g., *Albertson and Van Baelen*, 1970], and such an approach remains standard to this day [e.g., *Pirjola*, 2002]. Although any finite duration of a data time series can, in principle, be decomposed into a Fourier superposition of time-invariant sinusoids, a more suitable decomposition for a magnetic storm time series can be made in terms of initial conditions and transient exponential moment functions that are the basis of the Laplace transform. Depending on solar wind conditions, some magnetic storms commence suddenly, others, more gradually; the energy of the magnetospheric-ionospheric system, as measured by ground-level magnetic disturbance, can grow and evolve, but, ultimately, there is a dissipative return to relative quiescence. For a nonstationary magnetic storm time series, then, it is important to preserve the property of time causality. By deriving needed mathematical formulas in the Laplace-transformed frequency domain, it is possible to obtain an estimate of electric field induction in the time domain that is dependent only on past magnetic field variation. In this report, we use a time causal mathematical formalism in our investigation of the degree to which a very simple parameterization of lithospheric electrical conductivity can be used to estimate magnetic storm induction of geoelectric fields. Such a formalism might be implemented in an operational setting for real-time hazard monitoring.

## 2. Observatory Data

We use geomagnetic and geoelectric field time series data from the Kakioka observatory of the Japan Meteorological Agency [*Minamoto*, 2013]. The Kakioka observatory is part of the International Real-time Magnetic Observatory Network (INTERMAGNET) [e.g., *Love and Chulliat*, 2013], and as such, its magnetometers are operated according to modern international standards. Somewhat more unusual at Kakioka is the collection, for several decades now, of ground electric potentiometer data. The observatory is located (geographic coordinates: 36.23°N, 140.19°E) on the eastern side of the Japanese main island of Honshu, which is, itself, on the western back arc of the Japan Trench subduction zone. As a “low-latitude” observatory, Kakioka is well situated to record magnetic storm disturbance generated by the equatorial ring current of the inner magnetosphere.

The geomagnetic data were collected at Kakioka with a fluxgate sensor; the data have been calibrated for drift in sensor system response, and they are reported in geographic polar vector components ( $B_h$  horizontal intensity,  $B_d$  declination, and  $B_z$  down). The geoelectric data were collected by measuring the potential difference between pairs of grounded electrodes oriented, respectively, along north-south and east-west lines and separated by 190 m; the data are reported in geographic Cartesian vector components  $\mathbf{E} = (E_x \text{north}, E_y \text{east})$ ; no measurements were made of the geoelectric vertical component. For intercomparison, we convert the magnetic data to Cartesian components. We invoke the plane-wave approximation, standard in magnetotellurics [*Stratton*, 1941, section 9.8; *Chave and Weidelt*, 2012, pp. 26–36] and consider only horizontal-component time dependence; therefore, henceforth,  $\mathbf{B} = (B_x, B_y)$ .

We analyze 1 s data values from Kakioka. These amount to instantaneous “spot” measurements of natural and continuous magnetic and electric field variation. All the data values can be represented as discrete sequences,  $\mathbf{B}^m(t_i)$  and  $\mathbf{E}^m(t_i)$ , for time-stamp values  $t_i, t_{i+1}, t_{i+2}, \dots$ , where  $\tau = t_{i+1} - t_i$  is the constant 1 s sampling interval. For convenience of plotting, we subtract a constant baseline from the magnetic data; this does not affect our results. The electric field data contain a slow drift in baseline that is an artifact of changes in electrode grounding [e.g., *Ferguson*, 2012, pp. 430–431]. This is not relevant to our analysis, and so we subtract a linear trend line. The data are almost complete in time; we fill a few gaps and replace a few locked values by linear interpolation.

## 3. Halloween Magnetic Storm

We analyze Kakioka data covering the 3 day (72 h) duration 29 October to 31 October 2003 [e.g., *Gopalswamy et al.*, 2005] which records the so-called Halloween storm; see Figure 1. Following over a week of enhanced solar activity, this storm commenced with the arrival at Earth of a solar wind shock wave from a coronal mass ejection. This abruptly compressed the magnetopause, generating a positive magnetic impulse in  $B_x$  (Figure 1a, blue) and a negative induced impulse in  $E_y$  (Figure 1c, black) each at 06:13 UT 29 October. This was followed by about 12 h of jumbled interplanetary magnetic field and variable solar wind

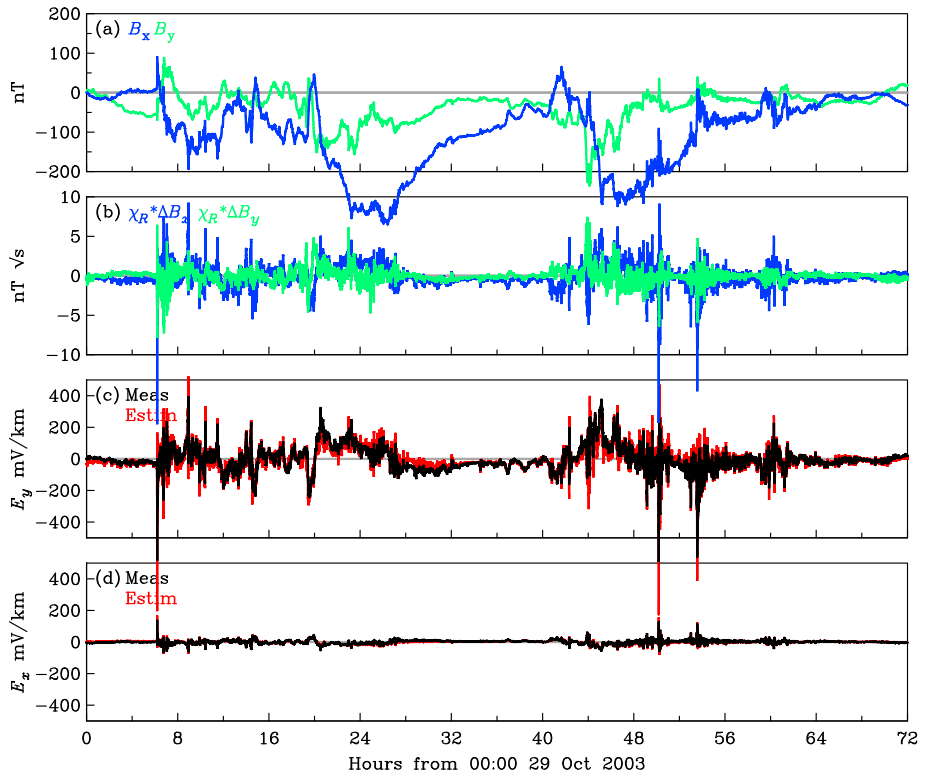


**Figure 1.** Time series of Kakioka 1 s data showing (a) magnetic storm variation,  $B_x$  (blue) and  $B_y$  (green) (b) inductional convolution,  $\chi_R * \Delta B_x$  (blue) and  $\chi_R * \Delta B_y$  (green), (c) electric field variation,  $E_y$ , measured (black) and estimated (red), (d) electric field variation,  $E_x$ , measured (black) and estimated (red), all for 29 October to 31 October 2003.

velocity and, correspondingly, activity in Kakioka **B** and **E**. When the interplanetary magnetic field at Earth finally became more consistently southward, this led to about 8 h of strong magnetospheric convection. This resulted in main phase intensification of the ring current and a corresponding decrease in north-south magnetic field strength at Kakioka, with a minimum  $B_x$  occurring at 02:27 UT 30 October. The arrival of additional coronal mass ejections and a complex pattern of magnetospheric convection led to a second main phase such as is sometimes seen in large magnetic storms. The Halloween storm disrupted numerous technological systems around the world [Balch et al., 2004], and, in particular, it caused measurable operational stress in the Swedish [Pulkkinen et al., 2005] and Scottish power grids [Thomson et al., 2005].

#### 4. Forward Modeling of Induction

We construct a simple model of magnetic storm induction of electric fields in the lithosphere underneath an observatory. For this, it is natural to consider an idealized “flat Earth” model having Cartesian geometry, and where a unit positional vector is given by  $\hat{x} = (\hat{x}, \hat{y}, \hat{z})$ . The Earth’s surface is represented by the plane  $z=0$ ; the lithosphere is, for now, assumed to be an infinite half-space ( $z>0$ ) of uniform electrical conductivity; and everything above the Earth’s surface ( $z<0$ ) is assumed to be an insulator. We consider magnetic field variation occurring over time scales of seconds to days and induction within the solid Earth over lithospheric depth scales of a hundred or so kilometers. In this setting, we invoke the quasistatic approximation and neglect displacement currents in Maxwell’s equations. The time evolution of the magnetic field **B** in a uniformly conducting medium is, then, given by the diffusion equation,

$$\nabla^2 \mathbf{B} - \mu\sigma\partial_t \mathbf{B} = 0, \quad (1)$$

where  $t$  denotes time,  $\sigma$  is electrical conductivity, and  $\mu$  is magnetic permeability. The relationship between the time dependence of a magnetic field and its related electric field **E** is given by Faraday’s law,

$$\nabla \times \mathbf{E} + \partial_t \mathbf{B} = 0. \quad (2)$$

Under the plane-wave approximation and as a consequence of equations (1) and (2), field variation amplitudes have an exponential dependence with depth like  $e^{-kz}$ , where  $1/k$  is the characteristic spatial depth scale. We have

$$\mathbf{B}(t, z) = \mathbf{B}_0(z) + \mathbf{B}(t, 0)e^{-kz}; \quad \mathbf{E}(t, z) = \mathbf{E}(t, 0)e^{-kz}, \quad (3)$$

each for  $z > 0$ . We denote as  $\mathbf{B}_0$  the part of the magnetic field that changes slowly in time compared to the 3 day duration of time considered here; we approximate it as time steady, and we note that it will not affect our analysis.

We use Laplace transforms to work with the time dependence in the differential equations [e.g., *Butkov*, 1968, chapters 5 and 8]. After some initial moment ( $t \geq 0$ ), a signal  $f(t)$  is treated as the superposition of exponential "moments", and so the Laplace transformation from the time domain into the Laplace domain is given by

$$f(s) = \mathcal{L}\{f(t)\} = \int_0^{\infty} f(t)e^{-st}dt, \quad (4)$$

where  $s$  is a complex (real and imaginary) frequency. Inverse transformation back to the time domain is given by

$$f(t) = \mathcal{L}^{-1}\{f(s)\} = \frac{1}{2\pi i} \int_{\gamma-i\infty}^{\gamma+i\infty} f(s)e^{st}ds, \quad (5)$$

where  $i = \sqrt{-1}$  and where integration is along a contour in the complex  $s$ -plane with the positive real number  $\gamma$  chosen so as to ensure integral convergence. Calculating an inverse Laplace transform using Cauchy's residue theorem sometimes requires the discovery of a "keyhole" contour path that circumvents singularities, but many inverse transformations can be found in reference books [e.g., *Abramowitz and Stegun*, 1965, Chapter 29].

The Laplace transform of the time derivative of a function is useful,

$$\mathcal{L}\{\partial_t f(t)\} = sf(s), \quad (6)$$

where the preresponse boundary condition is assumed to be zero. With this and (3), the magnetic diffusion equation (1) can be reduced to an algebraic equation,

$$k^2 \mathbf{B} - s\mu\sigma \mathbf{B} = 0 \quad \text{or, more simply, } k^2 - s\mu\sigma = 0, \quad (7)$$

which is a characteristic polynomial. Next, with (3) and after making a Laplace transformation, Faraday's Law (2) reduces to the matrix equation

$$-k\mathbf{CE}(s) + s\mathbf{B}(s) = 0, \quad \text{where } \mathbf{C} = \begin{pmatrix} 0 & -1 \\ 1 & 0 \end{pmatrix} \quad (8)$$

is a spin matrix that comes from the curl operator and is only two-dimensional because we have invoked the plane-wave approximation. With the characteristic equation (7), we can write this as

$$\mathbf{CE}(s) = \frac{1}{\sqrt{\mu\sigma}} Z(s) \cdot \mathbf{B}(s), \quad (9)$$

where we define a pseudoimpedance (independent of  $\sigma$ )

$$Z(s) = \sqrt{s}. \quad (10)$$

Next, we recognize that multiplication in the Laplace domain corresponds to convolution in the time domain, so that for two functions  $f$  and  $g$ ,

$$f(s) \cdot g(s) = \mathcal{L}\{(f * g)(t)\}, \quad (11)$$

[e.g., *Butkov*, 1968, chapter 5.6]. With this, then, we consider the induction of an electric field by the time rate of change in a magnetic field,

$$\mathbf{CE}(s)|_D = \frac{1}{\sqrt{\mu\sigma}} \chi_D(s) \cdot \mathcal{L}\{\partial_t \mathbf{B}(t)\}, \quad (12)$$

where we define the time derivative transfer function

$$\chi_D(s) = \frac{Z(s)}{s} = \frac{1}{\sqrt{s}}. \quad (13)$$

With the convolution theorem, in the time domain we have

$$\mathbf{CE}(t; \sigma)|_D = \frac{1}{\sqrt{\mu\sigma}} (\chi_D * \partial_t \mathbf{B})(t). \quad (14)$$

With inverse Laplace transformation,

$$\chi_D(t) = \mathcal{L}^{-1}\left\{\frac{1}{\sqrt{s}}\right\} = \frac{1}{\sqrt{\pi t}}, \quad (15)$$

and with the integral expression of convolution,

$$(f * g)(t) = \int_0^t f(t - \theta) \cdot g(\theta) d\theta. \quad (16)$$

we obtain

$$\mathbf{CE}(t; \sigma)|_D = \frac{1}{\sqrt{\pi\mu\sigma}} \int_0^t \partial_t \mathbf{B}(\theta) \cdot \frac{d\theta}{\sqrt{t - \theta}}. \quad (17)$$

This is the classic equation given by *Cagniard* [1953, equation (12)]. He did not show its derivation and, indeed, he was not even interested in using it. Subsequently, however, other scientists have become interested in using (17) to make model estimates of induced electric fields from magnetic field data [e.g., *Pirjola*, 2002], but the square root in the denominator of (17) has a singularity at  $t = 0$ . This is an artifact of the quasistatic approximation in which displacement currents are ignored [e.g., *Pirjola*, 1984, p. 93]. It also represents a practical challenge. For discrete data samples recording a magnetic storm that begins (say) with a characteristic abrupt sudden commencement change in  $B_x$ , and as might be approximated by an impulse, how should the singularity in equation (17) at  $t = 0$  be handled?

We avoid this question by considering a slightly different model of the time evolution of the magnetic field: linear interpolation between discrete data values. For this we need the Laplace transform of a linear “ramp” function and, also, a linear ramp function that is delayed by time  $\tau$ ,

$$\mathcal{L}\{t\} = \frac{1}{s^2} \quad \text{and} \quad \mathcal{L}\{tH(t - \tau)\} = \frac{1}{s^2} e^{-\tau s}, \quad (18)$$

where the Heaviside step function is defined as

$$H(t - \tau) = \begin{cases} 0 & \text{for } t < \tau \\ 1 & \text{for } t > \tau \end{cases} \quad (19)$$

We obtain the transfer function for an inducing linear change in magnetic field over duration  $\tau$  by subtracting the Laplace transform of the  $\tau$ -delayed ramp function from that with no delay,

$$\chi_R(s; \tau) = \frac{1}{s^2} [1 - e^{-\tau s}] Z(s). \quad (20)$$

With inverse Laplace transformation, and using

$$\mathcal{L}^{-1}\left\{s^{-\frac{3}{2}}\right\} = 2\sqrt{\frac{t}{\pi}} \quad \text{and} \quad \mathcal{L}^{-1}\left\{s^{-\frac{3}{2}} e^{-\tau s}\right\} = 2\sqrt{\frac{t - \tau}{\pi}}, \quad (21)$$

we obtain the time domain form of the transfer function,

$$\chi_R(t; \tau) = \frac{2}{\sqrt{\pi}} \left[ \sqrt{t} H(t) - \sqrt{t - \tau} H(t - \tau) \right]. \quad (22)$$

*Pirjola* [1984, equation (7)] obtained a closely related result, but whereas he was interested in electric field response during a time linear change in magnetic field, we are interested in electric field response after a finite duration, time linear change in magnetic field. With discrete data time series,

$$\frac{\Delta \mathbf{B}(t_i)}{\tau} = \frac{\mathbf{B}(t_{i+1}) - \mathbf{B}(t_i)}{\tau}, \quad (23)$$

discrete values of the induced electric field, denoted  $\mathbf{E}(t_i)$ , are obtained by discrete linear convolution with the ramp transfer function (22),

$$\mathbf{CE}(t_i; \sigma)|_R = \frac{1}{\sqrt{\mu\sigma}} \left( \chi_R * \frac{\Delta \mathbf{B}}{\tau} \right) (t_i), \quad (24)$$

which can be compared with equation (14). We write this more explicitly as

$$\mathbf{CE}(t_i; \sigma)|_R = \frac{1}{\sqrt{\mu\sigma}} \sum_{j=1}^i \chi_R(t_i - t_j) \cdot \frac{\Delta \mathbf{B}(t_j)}{\tau}. \quad (25)$$

This formula does not have a singularity in time, and it is straightforward to use it with actual data.

## 5. Convolution Results

Before we continue, it is instructive to first examine the convolution part of equation (24), that is,  $(\chi_R * \Delta \mathbf{B})(t_i)$ . This is a time series that encapsulates the physical process of induction in the idealized half-space model of the lithosphere, but it is otherwise independent of any specific lithospheric conductivity. Convolution results for  $B_x^m$  and  $B_y^m$  are shown in Figure 1b (blue and green). We note, right away, that there is a generally proportional resemblance between  $\chi_R * \Delta B_x^m$  and  $E_y^m(t_i)$ , Figure 1c (black), as might be expected for induction in a homogeneous medium. On the other hand, the relationship between  $\chi_R * \Delta B_y^m$ , and  $E_x^m$ , Figure 1d (black), is not obvious, and since, generally speaking,  $|E_x| \ll |E_y|$ , any proportionality between  $\chi_R * \Delta B_y^m$  and  $E_x^m$  is certainly different from that between  $\chi_R * \Delta B_x^m$  and  $E_y^m$ . This means, very simply, that an idealized half-space model for lithospheric conductivity cannot adequately account for the physical relationship between storm time geomagnetic field variation and the induced geoelectric field at Kakioka. Indeed, even a 1-D vertically stratified conductivity model could not account for the inductional relationship recorded in the Kakioka data!

## 6. Electrical Conductivity and Distortion

We recognize, of course, that the Earth's electrical conductivity is a function of both geographic location and depth. At a radial depth of about 100 km, the conductivity of the upper mantle is approximately  $10^{-3}$  S/m; this increases to 1 S/m at the base of the mantle [e.g., *Utada et al.*, 2003]. Closer to the Earth's surface, within the lithosphere, conductivity has a much more complicated three-dimensional spatial distribution. From their magnetic sounding analysis of a two-dimensional transect across northern Honshu and eastward out into the Japan Trench, north of the Kakioka observatory, *Ogawa et al.* [1986] identified large spatial structures having low electrical conductivity,  $10^{-4}$  S/m, and other structures with higher conductivity,  $10^{-2}$  S/m, extending down below 100 km. These appear to be related to subduction of the Pacific plate underneath the Okhotsk plate. *Ogawa et al.* [1986] also identified some smaller conductivity structures,  $10^{-1}$  to 1 S/m at depths of about 30 km, that might be associated with volcanism. Their estimates of crustal conductivity structures range from  $10^{-2}$  to  $10^{-1}$  S/m. *Fuji-ta et al.* [1997] and *Kasaya et al.* [2005] identified spatial variation in conductivity of similar amounts in their analyses of magnetotelluric data. And, finally, we note that sea water is a very good conductor, 3.5 S/m.

Electric charges accumulate along the boundaries of spatial heterogeneities in lithospheric conductivity and within conductivity gradients. Localized charge separation sets up quasistatic electric fields that are not especially well correlated with electric fields generated by broader regional-scale induction. It is standard within the magnetotelluric community to model the measured electric field  $\mathbf{E}^m$  as a distortion of the calculated induced field  $\mathbf{E}$  using a time-constant galvanic tensor  $\mathbf{G}$  [e.g., *Groom and Bahr*, 1992; *Jones*, 2012],

$$\mathbf{E}^m(t_i) = \mathbf{GE}(t_i), \quad \text{where } \mathbf{G} = \begin{pmatrix} g_{xx} & g_{xy} \\ g_{yx} & g_{yy} \end{pmatrix}. \quad (26)$$

From the standpoint of our modeling project, this tensor represents free parameters that we need to constrain through analysis of observatory magnetic and electric field data. Toward that end, we use equations (24) and (26) to define the discrepancy between the measured electric field and the galvanic distortion of induction,

$$\mathbf{d}(t_i; \sigma, \mathbf{G}) = \mathbf{CE}^m(t_i) - \frac{1}{\sqrt{\mu\sigma}} \mathbf{G}(\chi_R * \Delta\mathbf{B}^m)(t_i), \quad (27)$$

where  $\mathbf{B}^m$  is the measured magnetic field. Since  $1/\sqrt{\mu\sigma}$  multiplies  $\mathbf{G}$ , we need to remove nonuniqueness in the parameterization. We do this by requiring the squared Frobenius norm  $\text{Tr}(\mathbf{GG}^T) = 2$ , in which case,  $\sigma$  can be interpreted as a geometrically averaged “effective” conductivity.

## 7. Estimation of Electric Fields

Using the magnetic and electric field data summarized in section 2, we estimate model parameters by least squares optimization, performing a separate optimization for each electric field component. For example, for  $E_x^m$  we minimize

$$\varepsilon_x^2 = \left( \sum_i (d_x(t_i))^2 \right) / \left( \sum_i (E_x^m(t_i))^2 \right). \quad (28)$$

We obtain

$$\sigma = 5.13 \times 10^{-4} \text{ S/m} \quad \text{and} \quad \mathbf{G} = \begin{pmatrix} 1.33 & 0.42 \\ -0.21 & 0.06 \end{pmatrix}. \quad (29)$$

This effective  $\sigma$  falls within the broad range of values determined by magnetic sounding and magnetotelluric analyses that we summarize in section 6. It is also compatible with laboratory-based measurements of the electrical conductivity of dry olivine, the most common mineral of the upper mantle, under representative conditions for temperature and pressure [e.g., Yoshino and Katsura, 2013].

With respect to the estimated parameters of the galvanic tensor  $\mathbf{G}$ , equation (29), these show significant electric field distortion. A simple half-space conductivity model alone, or, indeed, conductivity that is only depth dependent, with no lateral conductivity structure, would have no galvanic distortion, and  $\mathbf{G}$  would be the identity matrix. Such a simple tensor would not support mutual induction of each electric field component by both horizontal magnetic field components. But the galvanic tensor we obtain here from analysis of the Kakioka data has substantial cross coupling; the north-south electric field is actually mostly related to north-south magnetic field activity! The data are telling us that lithospheric conductivity in the vicinity of Kakioka is spatially complicated.

If we define “prediction efficiency” as  $1 - \varepsilon^2$ , then (29) accounts for 87% of the variance in the 1 s Kakioka  $\mathbf{E}^m$  data for the Halloween storm. In Figures 1c and 1d we compare the output model electric field (red) against the electric field (black) measured at Kakioka. Low-frequency electric field variation, with characteristic periods longer than an hour or so, is reasonably well fitted, but model high-frequency electric field variation is greater than that which was actually measured (red variance > black variance). Clearly, improved fits can be obtained by allowing for a depth-dependent conductivity (together with a galvanic tensor). Optimization to minimize the high-frequency misfit seen in Figures 1c and 1d would, almost certainly, be reduced, yielding a model with high conductivity near the surface, such as actually exists.

## 8. Real-Time Hazard Monitoring

Our analysis of transient and aperiodic magnetic storm time series using the Laplace transform leads to mathematical formulas that are strictly time causal. This is, of course, an important property for real-time operational estimation of storm time induction. But to implement our formulas, conductivity and galvanic parameters must be specified. Appropriate values can be estimated, for a specific observatory site, by fitting model electric fields to electric fields measured during a few magnetic storms. Since the physical properties of the lithosphere underneath an observatory change very slowly (over geological timescales), electric fields for future storms can be estimated with a measurable accuracy. If this accuracy, for a given observatory,

is deemed sufficient (for whatever purpose), then continued electric field measurement might be unnecessary; algorithmic estimates can be used instead. Electric field measurement systems might then be moved to a new site.

At the same time, we certainly support long-term, dedicated monitoring of geoelectric fields at as many reference observatories as is practically possible, such as those located near metropolitan areas with electric power grids that might be susceptible to induction hazards. As always, direct geophysical monitoring is essential for testing hypotheses that lead to improved fundamental understanding, for deriving products such as algorithms and maps that are needed for practical application, and for discovering new and unexpected natural phenomena.

### Acknowledgments

We thank C. A. Finn and E. J. Rigler for reviewing a draft manuscript. We thank C. Balch, W. D. Barnhart, A. Chulliat, J. L. Gannon, G. Hulot, A. Jackson, M. D. Jegen, S. I. Lotz, M. C. Nair, and H. J. Singer for useful conversations. This work was supported by the USGS Geomagnetism Program; part of this work was accomplished while J. J. Love was visiting the Institut de Physique du Globe de Paris, October 2013. The data for this paper are available from the JMA's Kakioka magnetic observatory, <http://www.kakioka-jma.go.jp>.

The Editor thanks two anonymous reviewers for their assistance in evaluating this paper.

### References

- Abramowitz, M., and I. A. Stegun (1965), *Handbook of Mathematical Functions*, 1046 pp., Dover, New York.
- Albertson, V. D., and J. A. Van Baelen (1970), Electric and magnetic fields at the Earth's surface due to auroral currents, *IEEE Trans. Power Appar. Syst.*, 89, 578–584.
- Baker, D. N., et al. (2008), *Severe Space Weather Events – Understanding Societal and Economic Impacts*, 144 pp., The National Acad. Press, Washington, D. C.
- Balch, C., B. Murtagh, D. Zezula, L. Combs, G. Nelson, K. Tegnell, M. Crown, and B. McGehan (2004), *Service Assessment: Intense Space Weather Storms October 19 – November 07, 2003*, 49 pp., U.S. Dep. of Commer., NOAA, Silver Spring, Md.
- Beggan, C. D., D. Beamish, A. Richards, G. S. Kelly, and A. W. P. Thomson (2013), Prediction of extreme geomagnetically induced currents in the UK high-voltage network, *Space Weather*, 11, 407–419, doi:10.1002/swe.20065.
- Bolduc, L. (2002), GIC observations and studies in the Hydro-Québec power system, *J. Atmos. Sol. Terr. Phys.*, 64, 1793–1802.
- Boteler, D. H., R. J. Pirjola, and H. Nevanlinna (1998), The effects of geomagnetic disturbances on electrical systems at the Earth's surface, *Adv. Space Res.*, 22, 17–27.
- Butkov, E. (1968), *Mathematical Physics*, 735 pp., Addison-Wesley, New York.
- Cagniard, L. (1953), Basic theory of the magneto-telluric method of geophysical prospecting, *Geophysics*, 18, 605–635.
- Chave, A. D., and A. G. Jones (Eds.) (2012), *The Magnetotelluric Method*, Cambridge Univ. Press, Cambridge, U. K.
- Chave, A. D., and P. Weidelt (2012), The theoretical basis for electromagnetic induction, in *The Magnetotelluric Method*, edited by A. D. Chave and A. G. Jones, pp. 19–49, Cambridge Univ. Press, Cambridge, U. K.
- Cowley, S. W. H. (1995), The Earth's magnetosphere: A brief beginner's guide, *EOS Trans. AGU*, 76(51), 525–529, doi:10.1029/95EO00322.
- Daglis, I. A. (Ed.) (2004), *Effects of Space Weather on Technology Infrastructure*, 334 pp., Kluwer Acad., Dordrecht, Netherlands.
- Ferguson, I. J. (2012), Instrumentation and field procedure, in *The Magnetotelluric Method*, edited by A. D. Chave and A. G. Jones, pp. 421–479, Cambridge Univ. Press, Cambridge, U. K.
- Fuji-ta, K., Y. Ogawa, S. Yamaguchi, and K. Yaskawa (1997), Magnetotelluric imaging of the SW Japan forearc—A lost paleoland revealed?, *Phys. Earth Planet. Inter.*, 102, 231–238.
- Gopalswamy, N., L. Barbieri, E. W. Cliver, G. Lu, S. P. Plunkett, and R. M. Skoug (2005), Introduction to violent Sun-Earth connection events of October–November 2003, *J. Geophys. Res.*, 110, A09S00, doi:10.1029/2005JA011268.
- Groom, R. W., and K. Bahr (1992), Corrections for near surface effects: Decomposition of the magnetotelluric impedance tensor and scaling corrections for regional resistivities: A tutorial, *Surv. Geophys.*, 13, 341–379.
- Jones, A. G. (2012), Distortion of magnetotelluric data: Its identification and removal, in *The Magnetotelluric Method*, edited by A. D. Chave and A. G. Jones, pp. 219–302, Cambridge Univ. Press, Cambridge, U. K.
- Kappenman, J. G. (2005), An overview of the impulsive geomagnetic field disturbances and power grid impacts associated with the violent Sun-Earth connection events of 29–31 October 2003 and a comparative evaluation with other contemporary storms, *Space Weather*, 3, S08C01, doi:10.1029/2004SW000128.
- Kappenman, J. G. (2012), A perfect storm of planetary proportions, *Spectrum, IEEE*, 49, 26–31.
- Kasaya, T., T. Goto, H. Mikada, K. Baba, K. Suyehiro, and H. Utada (2005), Resistivity image of the Philippine Sea plate around the 1944 Tonankai earthquake zone deduced by marine and land MT surveys, *Earth Planets Space*, 57, 209–213.
- Korja, T. (2007), How is the European lithosphere imaged by magnetotellurics?, *Surv. Geophys.*, 28, 239–272, doi:10.1007/s10712-007-9024-9.
- Love, J. J., and A. Chulliat (2013), An international network of magnetic observatories, *Eos Trans. AGU*, 42, 373–384, doi:10.1002/2013EO420001.
- Love, J. J., and C. A. Finn (2011), The USGS Geomagnetism Program and its role in space weather monitoring, *Space Weather*, 9, S07001, doi:10.1029/2011SW000684.
- McPherron, R. L. (1991), Physical processes producing magnetospheric substorms and magnetic storms, in *Geomagnetism*, vol. 4, edited by J. A. Jacobs, pp. 593–739, Acad. Press, London, U. K.
- Minamoto, Y. (2013), Availability and access to data from Kakioka Magnetic Observatory, Japan, *Data Sci. J.*, 12, G30–G35.
- Ogawa, Y., T. Yukutake, and H. Utada (1986), Two-dimensional modelling of resistivity structure beneath the Tohoku District, Northern Honshu of Japan, by a finite element method, *J. Geomag. Geoelectr.*, 38, 45–79.
- Pirjola, R. (1984), Estimation of the electric field on the Earth's surface during a geomagnetic variation, *Geophysica*, 20, 89–103.
- Pirjola, R. (2002), Review on the calculation of surface electric and magnetic fields and of geomagnetically induced currents in ground-based technological systems, *Surv. Geophys.*, 23, 71–90.
- Prölls, G. W. (2004), *Physics of the Earth's Space Environment*, 513 pp., Springer-Verlag, Berlin, Germany.
- Pulkkinen, A., S. Lindahl, A. Viljanen, and R. Pirjola (2005), Geomagnetic storm of 29–31 October 2003: Geomagnetically induced currents and their relation to problems in the Swedish high-voltage power transmission system, *Space Weather*, 3, S08C03, doi:10.1029/2004SW000123.
- Pulkkinen, A., R. Pirjola, and A. Viljanen (2007), Determination of ground conductivity and system parameters for optimal modeling of geomagnetically induced current flow in technological systems, *Earth Planets Space*, 59, 999–1006.
- Pulkkinen, A., E. Bernabeu, J. Eichner, C. Beggan, and A. W. P. Thomson (2012), Generation of 100-year geomagnetically induced current scenarios, *Space Weather*, 10, S04003, doi:10.1029/2011SW000750.

- Simpson, F., and K. Bahr (2005), *Practical Magnetotellurics*, 254 pp., Cambridge Univ. Press, Cambridge, U. K.
- Stratton, J. A. (1941), *Electromagnetic Theory*, 615 pp., McGraw-Hill Book Company, New York.
- Thomson, A. W. P., A. J. McKay, E. Clarke, and S. J. Reay (2005), Surface electric fields and geomagnetically induced currents in the Scottish Power grid during the 30 October 2003 geomagnetic storm, *Space Weather*, 3, S11002, doi:10.1029/2005SW000156.
- Tsurutani, B. T., W. D. Gonzalez, Y. Kamide, and J. K. Arballo (Eds.) (1997), *Magnetic Storms*, *Geophys. Monogr. Ser.*, vol. 98, 266 pp., AGU, Washington, D. C.
- Utada, H., T. Koyama, H. Shimizu, and A. D. Chave (2003), A semi-global reference model for electrical conductivity in the mid-mantle beneath the north Pacific region, *Geophys. Res. Lett.*, 30(4), 1194, doi:10.1029/2002GL016092.
- Viljanen, A., R. Pirjola, M. Wik, A. Adám, E. Prácsér, Y. Sakharov, and J. Katkalov (2012), Continental scale modelling of geomagnetically induced currents, *J. Space Weather Space Clim.*, 2, A17, doi:10.1051/swsc/2012017.
- Watari, S., et al. (2009), Measurements of geomagnetically induced current in a power grid in Hokkaido, Japan, *Space Weather*, 7, S03002, doi:10.1029/2008SW000417.
- Wei, L. H., N. Homeier, and J. L. Gannon (2013), Surface electric fields for North America during historical geomagnetic storms, *Space Weather*, 11, 451–462, doi:10.1002/swe.20073.
- Yoshino, T., and T. Katsura (2013), Electrical conductivity of mantle minerals: Role of water in conductivity anomalies, *Ann. Rev. Earth Planet. Sci.*, 41, 605–628.